

The Mpemba effect in the Descartes protocol: A time-delayed Newton's law of cooling approach

Andrés Santos¹

¹Departamento de Física, Universidad de Extremadura, E-06006 Badajoz, Spain and Instituto de Computación Científica Avanzada (ICCAEx), Universidad de Extremadura, E-06006 Badajoz, Spain
(*andres@unex.es)

(Dated: February 4, 2026)

We investigate the direct and inverse Mpemba effects within the framework of the time-delayed Newton's law of cooling by introducing and analyzing the Descartes protocol, a three-reservoir thermal scheme in which each sample undergoes a single-step quench at different times. This protocol enables a transparent separation of the roles of the delay time τ , the waiting time t_w , and the normalized warm temperature ω , thus providing a flexible setting to characterize anomalous thermal relaxation. For instantaneous quenches, exact conditions for the existence of the Mpemba effect are obtained as bounds on ω for given τ and t_w . Within those bounds, the effect becomes maximal at a specific value $\omega = \tilde{\omega}(t_w)$, and its magnitude is quantified by the extremal value of the temperature-difference function at this optimum. Accurate and compact approximations for both $\tilde{\omega}(t_w)$ and the maximal magnitude $Mp(t_w)$ are derived, showing in particular that the absolute maximum at fixed τ is reached for $t_w = \tau$. A comparison with a previously studied two-reservoir protocol reveals that, despite its additional control parameter, the Descartes protocol yields a smaller maximal magnitude of the effect. The analysis is extended to finite-rate quenches, where strict equality of bath conditions prevents a genuine Mpemba effect, although an approximate one survives when the bath time scale is sufficiently short. The developed framework offers a unified and analytically tractable approach that can be readily applied to other multi-step thermal protocols.

I. INTRODUCTION

The Mpemba effect is the counterintuitive phenomenon in which, under certain conditions, a system initially prepared at a higher temperature relaxes to equilibrium faster than an identical system prepared at a lower temperature. Although qualitative observations date back to Aristotle [1], the effect was brought to modern scientific attention by the experiments of Mpemba and Osborne on water freezing [2]. For decades, it was considered a curiosity specific to water, with explanations invoking evaporation, convection, dissolved gases, or supercooling [3–19].

In recent years, however, the Mpemba effect has attracted renewed interest as a genuinely nonequilibrium phenomenon of broad relevance [20]. It has been theoretically predicted and experimentally observed in a variety of systems, including granular fluids [21–31], spin models [32–38], colloidal suspensions [39–43], Markov jump processes [36, 41, 44–47], and quantum systems [48–59]. This broader perspective has led to the identification of generalized and inverse Mpemba effects, as well as to a unifying theoretical framework based on the spectral properties of the relaxation dynamics. Consequently, the Mpemba effect is now recognized as a sensitive probe of nonequilibrium relaxation pathways, placing it at the forefront of current research in statistical mechanics and nonequilibrium thermodynamics [20].

A simple phenomenological framework for studying memory effects in thermal relaxation is provided by the

time-delayed Newton's cooling law [60–62]:

$$\dot{T}(t) = -\lambda [T(t - \tau) - T_b(t)]. \quad (1)$$

Here, λ is the heat transfer coefficient, $T_b(t)$ is the time-dependent temperature of the bath, and $0 < \tau < e^{-1} \simeq 0.368$ is the delay time. In this formulation, the system's temperature evolution depends on its past state rather than solely on its instantaneous deviation from the bath temperature, with the delay parameter τ playing a central role in capturing nontrivial thermal relaxation dynamics.

In two recent papers [61, 62], I analyzed the conditions under which Eq. (1) predicts a Mpemba effect between two samples (A and B) using only two reservoirs. The protocol was as follows: sample A was first thermalized at the hot temperature T_{hot} and then quenched to the cold temperature T_{cold} at $t = -t_w$. Sample B was initially thermalized at T_{cold} , quenched to T_{hot} at $t = -t_w$, and finally quenched again to T_{cold} at $t = 0$, resulting in a double-step quench of sample B. Hereafter, this scheme will be referred to as the two-reservoir protocol, to emphasize that only the extreme temperatures T_{hot} and T_{cold} are employed. Figure 1(a) schematically illustrates this protocol. Reference [61] showed that, for a given λ , the relevant parameter space is two-dimensional (delay time τ and waiting time t_w), and the Mpemba effect occurs only within a specific region of this plane.

A different two-step quench protocol, inspired by Aristotle's account of fishing habits in the Pontus region [1], has also been proposed [59, 63]. The Pontus protocol, shown in Fig. 1(b), begins by equilibrating both samples at a common warm temperature T_{warm} . At

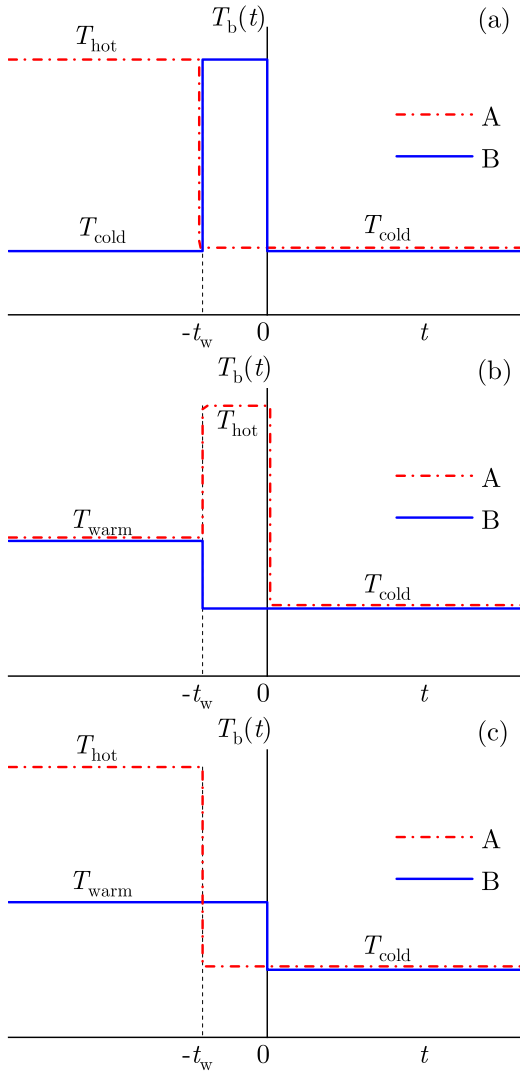


FIG. 1. Schematic representation of three protocols applied to samples A and B. Panel (a) depicts the two-reservoir protocol of Refs. [61, 62], where sample A undergoes a single-step quench at $t = -t_w$ and sample B a double-step quench at $t = -t_w$ and $t = 0$. Panel (b) illustrates the Pontus protocol, in which three thermal reservoirs are used: sample B undergoes a single-step quench and sample A a double-step quench. Panel (c) shows the Descartes protocol, where three reservoirs are again used but both samples undergo single-step quenches at $t = -t_w$ (sample A) and $t = 0$ (sample B).

time $t = -t_w$, sample A is quenched to T_{hot} and sample B to T_{cold} . Then, at $t = 0$, sample A undergoes a second quench to T_{cold} . In contrast to the two-reservoir protocol illustrated in Fig. 1(a), the Pontus protocol involves three different reservoirs.

An alternative and simpler protocol is sketched in Fig. 1(c). In this case, both samples undergo a single-step quench, and, as in the Pontus protocol, three temperatures (T_{hot} , T_{warm} , and T_{cold}) are involved. This preparation of samples A and B is reminiscent of Descartes' prescription [64]:

"In order to perform this experiment properly, the water must be allowed to cool down after it has boiled, until it has attained the same degree of coldness as water from a spring. After taking the temperature with a thermometer, you should take some water from a spring and pour equal quantities of the two sorts of water into identical vessels."

In this description, T_{hot} , T_{warm} , and T_{cold} correspond to the boiling temperature, the spring water temperature, and the freezing temperature of water, respectively. In Descartes' original experiment, the waiting time t_w is chosen such that $T_A(0) = T_B(0) = T_{\text{warm}}$. Here, however, we will treat t_w as a control parameter independent of T_{hot} , T_{warm} , and T_{cold} .

Throughout this paper, the protocol illustrated in Fig. 1(c) will be referred to as the Descartes protocol. The aim is to analyze this protocol within the framework of Eq. (1). As will be seen, the parameter space is three-dimensional: besides the delay time τ and the waiting time t_w , an additional control parameter is the *normalized warm temperature*

$$\omega \equiv \frac{T_{\text{warm}} - T_{\text{cold}}}{T_{\text{hot}} - T_{\text{cold}}}. \quad (2)$$

This dimensionless parameter represents the relative position of the intermediate temperature T_{warm} between the hot (T_{hot}) and cold (T_{cold}) temperatures, quantifying how close T_{warm} is to either extreme. It ranges from $\omega = 0$ (if $T_{\text{warm}} = T_{\text{cold}}$) to $\omega = 1$ (if $T_{\text{warm}} = T_{\text{hot}}$).

The paper is organized as follows. The Descartes protocol for the direct Mpemba effect is analyzed in detail in Sec. II, while the inverse Mpemba effect is considered in Sec. III. Section IV discusses the influence of finite-rate quenches. The paper concludes with a summary and outlook in Sec. V.

II. THE DESCARTES PROTOCOL FOR THE DIRECT MPEMBA EFFECT

For simplicity, we henceforth set $\lambda^{-1} = 1$ as the unit of time. Since the delay time τ is inherent to the delayed Newton's cooling law, Eq. (1), rather than to any particular solution, its explicit dependence will be omitted in the notation throughout this paper for clarity.

A. Solution of the time-delayed Newton's cooling equation

As illustrated in Fig. 1(c), in the Descartes cooling protocol, sample A remains in thermal equilibrium with a reservoir at the hot temperature T_{hot} until $t = -t_w$, when it is quenched to the cold temperature T_{cold} . Sample B, on the other hand, is equilibrated with a reservoir at the warm temperature T_{warm} until $t = 0$, when

it is also quenched to T_{cold} . If the initial post-quench temperatures satisfy $T_A(0) > T_B(0)$, a Mpemba effect occurs provided that the temperatures cross at some time $t_x > 0$, i.e., $T_A(t_x) = T_B(t_x)$, and subsequently satisfy $T_A(t) < T_B(t)$ for $t > t_x$.

From the general solution to Eq. (1) [62], the time evolution of the sample temperatures is

$$T_A(t) = \begin{cases} T_{\text{hot}}, & t \leq -t_w, \\ T_{\text{cold}} + (T_{\text{hot}} - T_{\text{cold}})\mathcal{E}(t + t_w), & t \geq -t_w, \end{cases} \quad (3a)$$

$$T_B(t) = \begin{cases} T_{\text{warm}}, & t \leq 0, \\ T_{\text{cold}} + (T_{\text{warm}} - T_{\text{cold}})\mathcal{E}(t), & t \geq 0, \end{cases} \quad (3b)$$

where $\mathcal{E}(t)$ is the quasi-exponential (τ -exp) function

$$\begin{aligned} \mathcal{E}(t) &= 1 + \sum_{n=0}^{\lfloor t/\tau \rfloor} \frac{(n\tau - t)^{n+1}}{(n+1)!}, \quad t \geq 0, \\ &= \begin{cases} 1 - t, & 0 \leq t \leq \tau, \\ 1 - t + \frac{(\tau-t)^2}{2}, & \tau \leq t \leq 2\tau, \\ 1 - t + \frac{(\tau-t)^2}{2} + \frac{(2\tau-t)^3}{3!}, & 2\tau \leq t \leq 3\tau, \\ \dots, & \dots \end{cases} \quad (4) \end{aligned}$$

with $\lfloor \cdot \rfloor$ denoting the floor function. Note that

$$\partial_t \mathcal{E}(t) = -\mathcal{E}(t - \tau), \quad (5)$$

with the convention $\mathcal{E}(t) = 1$ for $t \leq 0$.

For asymptotically long times [61, 62],

$$\mathcal{E}(t) \approx \frac{\kappa_0^{-1} e^{-\kappa_0 t}}{1 - \kappa_0 \tau} - \frac{\kappa_1^{-1} e^{-\kappa_1 t}}{\kappa_1 \tau - 1}, \quad t \gg 1, \quad (6)$$

where $\kappa_0 = -\tau^{-1} W_0(-\tau)$ and $\kappa_1 = -\tau^{-1} W_{-1}(-\tau)$, with $W_0(z)$ and $W_{-1}(z)$ being the principal and lower branches of the Lambert function [65]. These roots satisfy $1 < \kappa_0 < e \simeq 2.718 < \tau^{-1} < \kappa_1$. For long times, the first term on the right-hand side of Eq. (6) dominates, while the second term improves the accuracy of $\mathcal{E}(t)$ even at relatively short times.

For $t \geq 0$, Eqs. (3) yield

$$\theta_A(t) = \mathcal{E}(t + t_w), \quad \theta_B(t) = \omega \mathcal{E}(t), \quad t \geq 0, \quad (7)$$

in terms of the normalized temperature

$$\theta(t) \equiv \frac{T(t) - T_{\text{cold}}}{T_{\text{hot}} - T_{\text{cold}}}. \quad (8)$$

As an example, Fig. 2 shows the evolution of $\theta(t)$ for different choices of samples of types A and B. The genuine Descartes protocol, in which $T_A(0) = T_B(0) = T_{\text{warm}}$, corresponds to the pairs (A,B2) and (A2,B). The Mpemba crossover is observed in the cases (A,B3) and (A3,B).

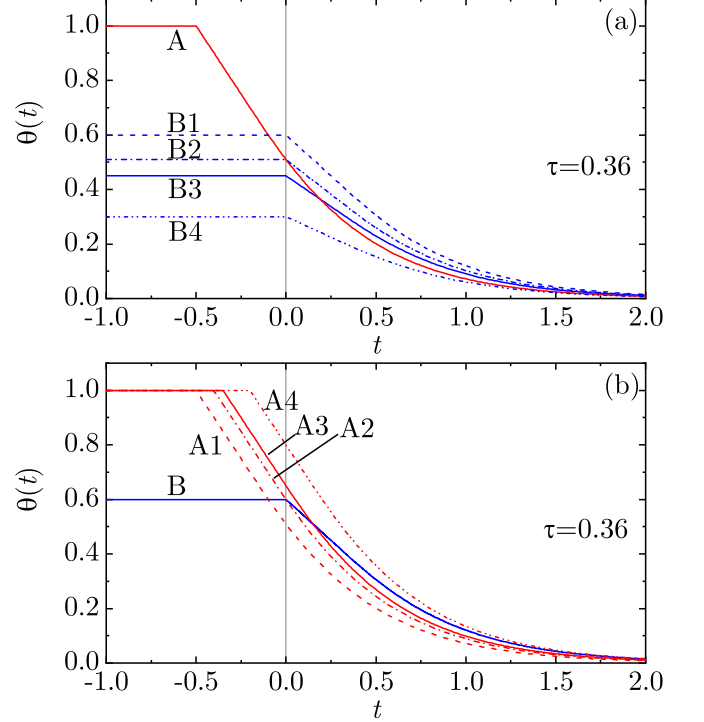


FIG. 2. Normalized temperature $\theta(t)$ for different samples of type A and type B with a delay time $\tau = 0.36$. In panel (a), the waiting time is $t_w = 0.5$ for sample A, while the normalized warm temperature is $\omega = 0.60, 0.51, 0.45$, and 0.30 in samples B1, B2, B3, and B4, respectively. In panel (b), the normalized warm temperature is $\omega = 0.60$ for sample B, while the waiting time is $t_w = 0.50, 0.40, 0.35$, and 0.20 in samples A1, A2, A3, and A4, respectively.

In the cases (A,B1) and (A1,B), the waiting time and/or the warm temperature are sufficiently large that $T_A(0) < T_B(0)$, preventing a Mpemba effect. Conversely, in the cases (A,B4) and (A4,B), the waiting time and/or the warm temperature are too small to allow sample A to catch up with sample B.

To analyze the conditions for the Mpemba effect, we define the difference function

$$\Delta(t; t_w, \omega) \equiv \theta_A(t) - \theta_B(t), \quad t \geq 0. \quad (9)$$

From Eq. (7), we then have

$$\Delta(t; t_w, \omega) = \mathcal{E}(t + t_w) - \omega \mathcal{E}(t), \quad (10)$$

whose time derivative satisfies

$$\partial_t \Delta(t; t_w, \omega) = -\Delta(t - \tau, t_w, \omega). \quad (11)$$

Notably, with the definitions in Eqs. (8) and (9), the difference function obtained from the two-reservoir protocol illustrated in Fig. 1(a) coincides exactly with twice the difference function of the Descartes protocol for the special case $\omega = 1/2$. Consequently, the results on the Mpemba effect reported in Refs. [61, 62] are recovered as a particular limit of the present analysis when $\omega = 1/2$.

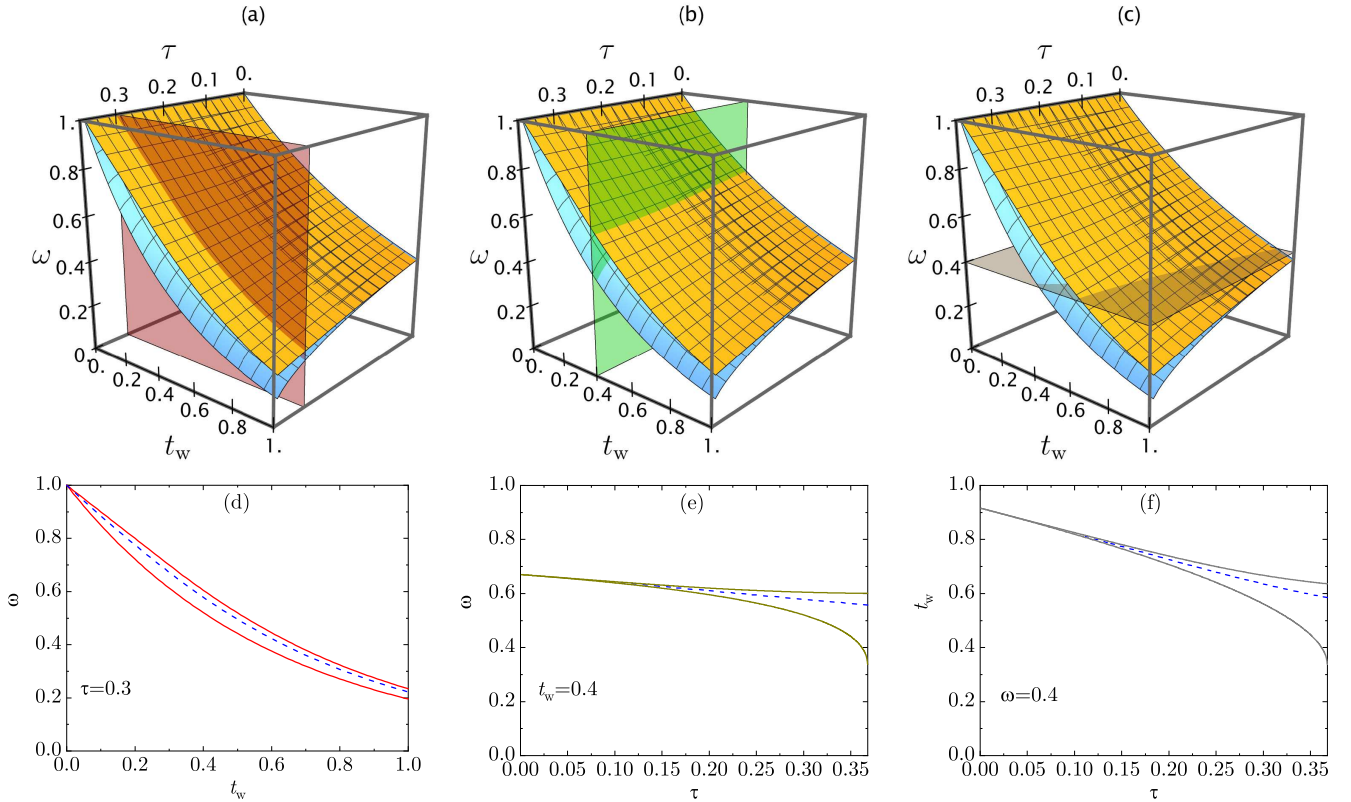


FIG. 3. Phase space for the direct Mpemba effect. In the top panels (a, b, c), the upper surface corresponds to the locus $\omega = E(t_w)$, while the lower surface represents $\omega = e^{-\kappa_0 t_w}$. The planes shown are (a) $\tau = 0.3$, (b) $t_w = 0.4$, and (c) $\omega = 0.4$. The region $\omega > E(t_w)$ is characterized by $\Delta(t \geq 0; t_w, \omega) < 0$, whereas $\Delta(t \geq 0; t_w, \omega) > 0$ holds in the region $\omega < e^{-\kappa_0 t_w}$. Consequently, a Mpemba effect occurs if and only if condition (14) is satisfied. Panels (d, e, f) show two-dimensional cross-sections of the three-dimensional phase space at $\tau = 0.3$, $t_w = 0.4$, and $\omega = 0.4$, respectively. Dashed lines indicate the loci where the Mpemba effect is maximal [see Sec. II C and Eq. (26)].

B. Conditions for the Mpemba effect

We now analyze the conditions for the existence of a Mpemba effect. The first basic requirement is $\Delta(0; t_w, \omega) > 0$, as occurs for the pairs (A,B3), (A,B4), (A3,B), and (A4,B) in Fig. 2. The second requirement is that $\Delta(t; t_w, \omega) < 0$ after a certain crossover time t_\times , as observed for the pairs (A,B3) and (A3,B).

At $t = 0$,

$$\Delta(0; t_w, \omega) = E(t_w) - \omega. \quad (12)$$

Hence, $\Delta(0; t_w, \omega) > 0$ if $\omega < E(t_w)$.

On the other hand, for long times, using Eq. (6),

$$\Delta(t; t_w, \omega) \approx (e^{-\kappa_0 t_w} - \omega) \frac{\kappa_0^{-1} e^{-\kappa_0 t}}{1 - \kappa_0 \tau}, \quad t \gg 1. \quad (13)$$

Therefore, $\Delta(t; t_w, \omega)$ approaches zero from below if $\omega > e^{-\kappa_0 t_w}$.

In summary, a Mpemba effect occurs if and only if the normalized warm temperature ω lies within the interval

$$e^{-\kappa_0 t_w} < \omega < E(t_w). \quad (14)$$

Using the relation $E(t) = 1 - t$ for $t < \tau$, this condition reduces, for small t_w , to

$$t_w < 1 - \omega < \kappa_0 t_w, \quad t_w \ll 1. \quad (15)$$

If condition (14) is satisfied, the difference function $\Delta(t; t_w, \omega)$ must vanish at a crossover time $t = t_\times(t_w, \omega)$, defined by

$$\omega = \frac{E(t_\times + t_w)}{E(t_\times)}. \quad (16)$$

This equation must generally be solved numerically. In the limiting case where ω is slightly below its upper bound $E(t_w)$, an approximate solution is

$$t_\times(t_w, \omega) \approx \frac{E(t_w)}{E(t_w - \tau) - E(t_w)} \left[1 - \frac{\omega}{E(t_w)} \right]. \quad (17)$$

The complementary case, where ω is slightly above its lower bound $e^{-\kappa_0 t_w}$, requires retaining both the leading and subleading terms in Eq. (6). After some algebra, the

resulting approximation is

$$t_{\times}(t_w, \omega) \approx \frac{1}{\kappa_1 - \kappa_0} \ln \left[\frac{1 - \kappa_0 \tau}{\kappa_1 \tau - 1} \frac{1 - e^{-(\kappa_1 - \kappa_0)t_w}}{\omega e^{\kappa_0 t_w} - 1} \right] - \tau. \quad (18)$$

After the crossover time, $-\Delta(t; t_w, \omega)$ reaches a maximum at a time $t_M(t_w, \omega)$, defined by $\partial_t \Delta(t; t_w, \omega) = 0$. Using Eq. (11), we have

$$t_M(t_w, \omega) = t_{\times}(t_w, \omega) + \tau. \quad (19)$$

The region in the three-dimensional parameter space τ, t_w, ω that satisfies Eq. (14) is illustrated in Figs. 3(a, b, c), while Figs. 3(d, e, f) show the corresponding two-dimensional projections obtained by intersecting this 3D space with the planes $\tau = 0.3$, $t_w = 0.4$, and $\omega = 0.4$, respectively.

The upper and lower surfaces in Figs. 3(a, b, c) meet along the lines $(t_w, \omega) = (0, 1)$ and $(\tau, \omega) = (0, e^{-\kappa_0 t_w})$. These intersections correspond to the points $(t_w, \omega) = (0, 1)$, $(\tau, \omega) = (0, 0.67)$, and $(\tau, t_w) = (0, 0.92)$ in Figs. 3(d, e, f), respectively.

For $\tau = 0.36$ and $t_w = 0.5$, the bounds of the Mpemba interval are $\omega = e^{-\kappa_0 t_w} \simeq 0.33$ and $\omega \simeq \mathcal{E}(t_w) \simeq 0.51$. This explains why a Mpemba effect is observed in Fig. 2(a) only for the case (A,B3). Similarly, for $\tau = 0.36$ and $\omega = 0.6$, the existence of a Mpemba effect requires $0.23 < t_w < 0.40$, justifying the crossover seen for the case (A3,B) in Fig. 2(b).

C. Optimal waiting time

Figure 3(d) shows that, for a fixed delay time τ , the width of the ω -interval,

$$\delta\omega(t_w) \equiv \mathcal{E}(t_w) - e^{-\kappa_0 t_w}, \quad (20)$$

vanishes in the limits $t_w \rightarrow 0$ and $t_w \rightarrow \infty$. Using Eqs. (6) and (15), one finds the asymptotic behavior

$$\delta\omega(t_w) \approx (\kappa_0 - 1)t_w, \quad t_w \ll 1, \quad (21a)$$

$$\delta\omega(t_w) \approx \left(\frac{\kappa_0^{-1}}{1 - \kappa_0 \tau} - 1 \right) e^{-\kappa_0 t_w}, \quad t_w \gg 1. \quad (21b)$$

This implies the existence of an *optimal* waiting time $t_w = t_w^{\text{opt}}$ that maximizes the width $\delta\omega(t_w)$. To determine it, note that

$$\partial_{t_w} \delta\omega(t_w) = \kappa_0 e^{-\kappa_0 t_w} - \mathcal{E}(t_w - \tau), \quad (22)$$

which vanishes at $t_w = \tau$. Hence, for a given delay time τ , the optimal waiting time is precisely

$$t_w^{\text{opt}} = \tau. \quad (23)$$

This resonance-like effect is illustrated in Fig. 4(a) for $\tau = 0.20, 0.30$, and 0.36 . The peak of $\delta\omega(t_w)$ at $t_w = \tau$

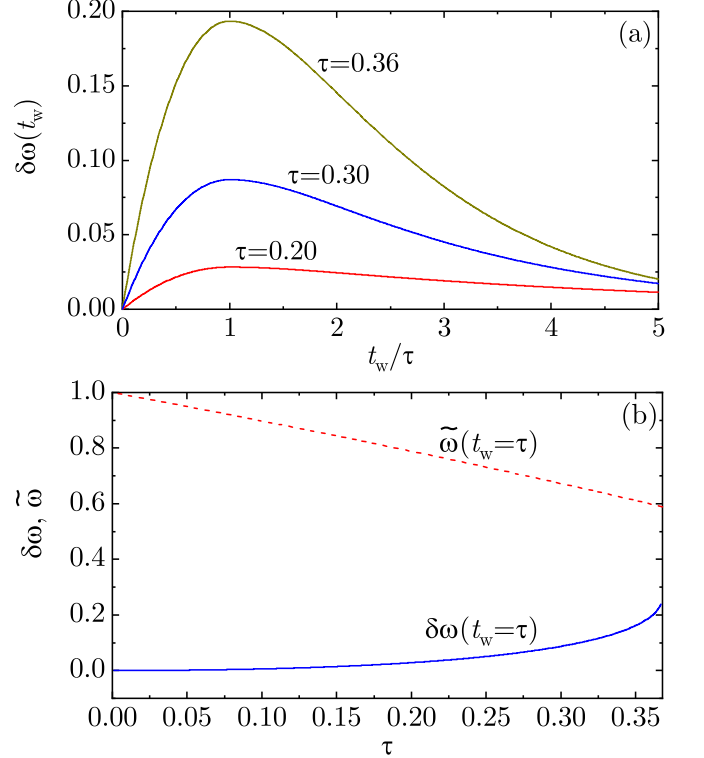


FIG. 4. (a) Width $\delta\omega(t_w)$ as a function of t_w/τ for $\tau = 0.20, 0.30$, and 0.36 . (b) Plot of $\delta\omega(t_w = \tau) = 1 - \tau - \kappa_0^{-1}$ and $\tilde{\omega}(t_w = \tau)$ [see Sec. II C and Eq. (37b)] versus τ .

becomes more pronounced as the delay time τ increases. The height of this peak is

$$\delta\omega(t_w = \tau) = 1 - \tau - \kappa_0^{-1}, \quad (24)$$

and is plotted in Fig. 4(b). Its maximum value, $1 - 2e^{-1} \simeq 0.264$, occurs at $\tau = \tau_{\text{max}} = e^{-1}$.

D. Magnitude of the Mpemba effect

1. Maximal effect

After identifying the Mpemba region in parameter space, the next step is to assess the magnitude of the effect. If ω is only slightly smaller than $\mathcal{E}(t_w)$, the Mpemba effect is weak: $T_A(0)$ is only marginally larger than $T_B(0)$, the crossover occurs at very short times [see Eq. (17)], and the temperature curves $T_A(t)$ and $T_B(t)$ remain close throughout the evolution. Conversely, if ω is only slightly larger than $e^{-\kappa_0 t_w}$, the effect is also weak because the crossover occurs at long times [see Eq. (18)], when both $T_A(t)$ and $T_B(t)$ have nearly equilibrated with the bath temperature T_{cold} .

Given two of the three free parameters (τ , t_w , and ω), the effect is maximized when the maximum positive and minimum negative values of $\Delta(t; t_w, \omega)$ are equal in

magnitude (but opposite in sign), i.e.,

$$\Delta(0; t_w, \omega) = -\Delta(t_x(t_w, \omega) + \tau; t_w, \omega), \quad (25)$$

as proposed in Ref. [61]. This condition for the *maximal* Mpemba effect leads to

$$\omega = \frac{\mathcal{E}(t_w) + \mathcal{E}(t_x(t_w, \omega) + \tau + t_w)}{1 + \mathcal{E}(t_x(t_w, \omega) + \tau)}. \quad (26)$$

The curves defined by Eq. (26) are plotted as dashed lines in Figs. 3(d, e, f). Notably, the surface described by Eq. (26) lies closer to the upper surface in Figs. 3(a, b, c) than to the lower surface.

For given τ and t_w , let $\tilde{\omega}(t_w)$ denote the solution to Eq. (26), and let $\tilde{t}_x(t_w) \equiv t_x(t_w, \tilde{\omega}(t_w))$ denote the corresponding crossover time. It can be observed that $\tilde{t}_x(t_w) < \tau$, so that, using Eq. (4),

$$\mathcal{E}(\tilde{t}_x(t_w)) = 1 - \tilde{t}_x(t_w), \quad (27a)$$

$$\mathcal{E}(\tilde{t}_x(t_w) + \tau) = 1 - \tau - \tilde{t}_x(t_w) + \frac{\tilde{t}_x^2(t_w)}{2}. \quad (27b)$$

As a consequence, Eqs. (16) and (26) yield

$$\frac{\mathcal{E}(\tilde{t}_x(t_w) + t_w)}{1 - \tilde{t}_x(t_w)} = \frac{\mathcal{E}(t_w) + \mathcal{E}(\tilde{t}_x(t_w) + \tau + t_w)}{2 - \tau - \tilde{t}_x(t_w) + \tilde{t}_x^2(t_w)/2}, \quad (28a)$$

$$\tilde{\omega}(t_w) = \frac{\mathcal{E}(\tilde{t}_x(t_w) + t_w)}{1 - \tilde{t}_x(t_w)}. \quad (28b)$$

Equation (28a) is a closed equation for $\tilde{t}_x(t_w)$ that can be solved numerically. Substituting the solution into Eq. (28b) then provides the optimal value of the normalized warm temperature, $\tilde{\omega}(t_w)$.

Figures 5(a) and 5(b) illustrate the dependence of $\tilde{\omega}(t_w)$ and $\tilde{t}_x(t_w)$, respectively, on the waiting time t_w for $\tau = 0.20, 0.30$, and 0.36 . As t_w increases, $\tilde{\omega}(t_w)$ decreases toward zero, while $\tilde{t}_x(t_w)$ approaches a well-defined plateau

$$\hat{t}_x \equiv \lim_{t_w \rightarrow \infty} \tilde{t}_x(t_w). \quad (29)$$

Using Eqs. (6) and (21b), one finds

$$\frac{e^{-\kappa_0 \hat{t}_x}}{1 - \hat{t}_x} = \frac{1 + \kappa_0^{-1} e^{-\kappa_0 \hat{t}_x}}{2 - \tau - \hat{t}_x + \hat{t}_x^2/2}, \quad (30a)$$

$$\tilde{\omega}(t_w) \approx \frac{\kappa_0^{-1}}{1 - \kappa_0 \tau} \frac{e^{-\kappa_0(\hat{t}_x + t_w)}}{1 - \hat{t}_x}, \quad t_w \gg 1, \quad (30b)$$

$$\lim_{t_w \rightarrow \infty} \frac{\tilde{\omega}(t_w)}{\delta \omega(t_w)} = \frac{1}{1 - \kappa_0(1 - \kappa_0 \tau)} \frac{e^{-\kappa_0 \hat{t}_x}}{1 - \hat{t}_x}. \quad (30c)$$

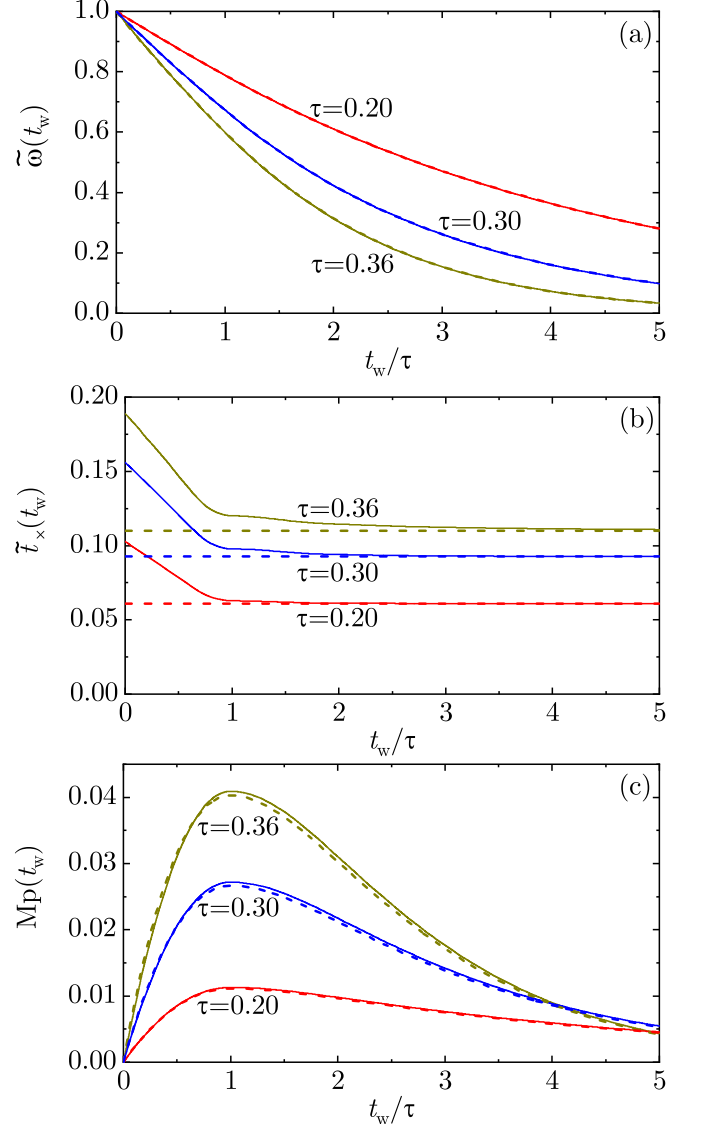


FIG. 5. Plots of (a) the optimal normalized warm temperature $\tilde{\omega}(t_w)$, (b) the corresponding crossover time $\tilde{t}_x(t_w)$, and (c) the magnitude of the Mpemba effect, $\text{Mp}(t_w)$, all as functions of t_w/τ for $\tau = 0.20, 0.30$, and 0.36 . In each panel, the dashed lines show the approximate results obtained from Eqs. (36), (30a), and (35), respectively.

2. Quantifying the magnitude of the effect

For given τ and t_w , Eqs. (28) determine the value $\tilde{\omega}(t_w)$ that maximizes the Mpemba effect in the sense that the minimum negative value of $\Delta(t; t_w, \omega)$ is equal in magnitude to its maximum positive value. We take this common absolute value as a measure of the Mpemba effect, denoted hereafter by $\text{Mp}(t_w)$. Using Eq. (12), this is simply

$$\text{Mp}(t_w) = \mathcal{E}(t_w) - \tilde{\omega}(t_w). \quad (31)$$

Figure 5(c) shows $\text{Mp}(t_w)$ for $\tau = 0.20, 0.30$, and 0.36 .

The magnitude exhibits a nonmonotonic dependence on the waiting time t_w . In the limit $t_w \rightarrow \infty$, one finds

$$\lim_{t_w \rightarrow \infty} \frac{\text{Mp}(t_w)}{\tilde{\omega}(t_w)} = (1 - \hat{t}_x) e^{\kappa_0 \hat{t}_x} - 1. \quad (32)$$

A striking qualitative similarity with Fig. 4(a) is apparent: both $\delta\omega(t_w)$ and $\text{Mp}(t_w)$ reach their maximum at $t_w = \tau$. To make this connection more precise, note that from Eqs. (30c) and (32), one obtains

$$\lim_{t_w \rightarrow \infty} \frac{\text{Mp}(t_w)}{\delta\omega(t_w)} = \frac{1 - e^{-\kappa_0 \hat{t}_x}}{1 - \kappa_0(1 - \kappa_0 \tau)}. \quad (33)$$

The right-hand side of Eq. (33) provides an excellent approximation for all t_w , particularly for smaller values of τ .

A further simplification is obtained by formally taking $\hat{t}_x \rightarrow 0$ on the right-hand side of Eq. (30a), which allows the approximation

$$\frac{e^{-\kappa_0 \hat{t}_x}}{1 - \hat{t}_x} \rightarrow \frac{1 + \kappa_0^{-1}}{2 - \tau}. \quad (34)$$

This leads to the compact expression

$$\begin{aligned} \text{Mp}(t_w) &\simeq \frac{1 - \tau - \kappa_0^{-1}}{2 - \tau} \frac{\delta\omega(t_w)}{1 - \kappa_0(1 - \kappa_0 \tau)} \\ &= \frac{1 - \tau - \kappa_0^{-1}}{2 - \tau} \frac{\mathcal{E}(t_w) - e^{-\kappa_0 t_w}}{1 - \kappa_0(1 - \kappa_0 \tau)}, \end{aligned} \quad (35)$$

which does not require solving Eq. (30a).

Inserting this result into Eq. (31) immediately yields an approximate expression for the optimal normalized warm temperature,

$$\tilde{\omega}(t_w) \simeq \mathcal{E}(t_w) - \frac{1 - \tau - \kappa_0^{-1}}{2 - \tau} \frac{\mathcal{E}(t_w) - e^{-\kappa_0 t_w}}{1 - \kappa_0(1 - \kappa_0 \tau)}. \quad (36)$$

As seen in Fig. 5(a), Eq. (36) provides an excellent approximation for $\tilde{\omega}(t_w)$, while Fig. 5(c) shows that Eq. (35) accurately captures the magnitude of the Mpemba effect.

Out of all possible waiting times at fixed τ , the maximum of $\text{Mp}(t_w)$ is reached at $t_w = \tau$. In this case, Eqs. (35) and (36) simplify to

$$\text{Mp}(t_w = \tau) \simeq \frac{(1 - \tau - \kappa_0^{-1})^2}{(2 - \tau)[1 - \kappa_0(1 - \kappa_0 \tau)]}, \quad (37a)$$

$$\tilde{\omega}(t_w = \tau) \simeq 1 - \tau - \frac{(1 - \tau - \kappa_0^{-1})^2}{(2 - \tau)[1 - \kappa_0(1 - \kappa_0 \tau)]}. \quad (37b)$$

Here we have used the properties $\mathcal{E}(\tau) = 1 - \tau$ and $e^{-\kappa_0 \tau} = \kappa_0^{-1}$. The function $\tilde{\omega}(t_w = \tau)$ is plotted in Fig. 4(b).

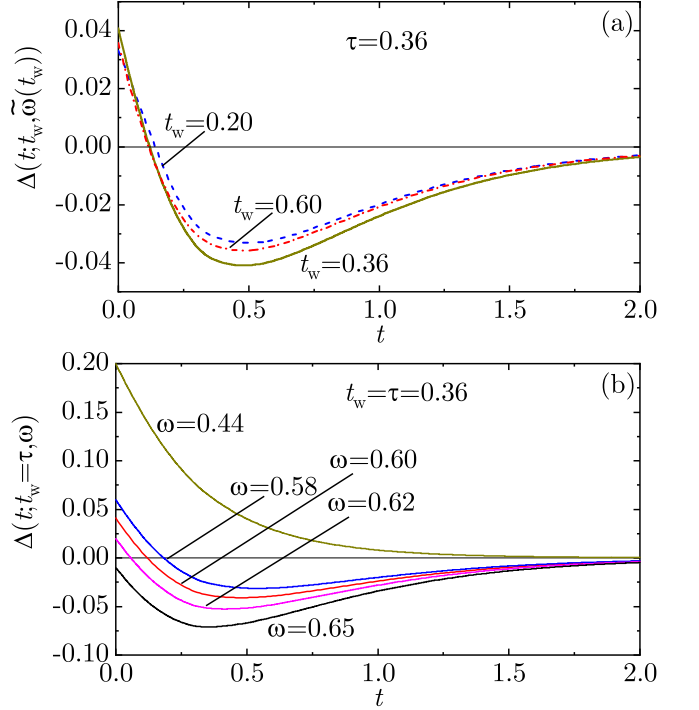


FIG. 6. (a) $\Delta(t; t_w, \omega)$ for $\tau = 0.36$ and three waiting times: $t_w = 0.20$, 0.36, and 0.60. In each case, the normalized warm temperature is set to $\omega = \tilde{\omega}(t_w) \simeq 0.77$, 0.60, and 0.39, respectively, ensuring that the maximum positive and minimum negative values of $\Delta(t; t_w, \omega)$ are equal in magnitude. The corresponding magnitudes of the Mpemba effect are approximately $\text{Mp}(t_w) = 0.033$, 0.041, and 0.036. (b) $\Delta(t; t_w, \omega)$ for $\tau = t_w = 0.36$ and five values of the normalized warm temperature: $\omega = 0.44$, 0.58, 0.60, 0.62, and 0.65. Note that $\tilde{\omega}(\tau = 0.36) \simeq 0.60$.

The advantage of selecting $t_w = \tau$ to maximize the Mpemba effect is illustrated in Fig. 6. Figure 6(a) shows $\Delta(t; t_w, \omega)$ for a delay time $\tau = 0.36$ and three waiting times ($t_w = 0.20$, 0.36, and 0.60), with the normalized warm temperature set to $\omega = \tilde{\omega}(t_w)$ in each case. In all three cases, the maximum positive and minimum negative values of $\Delta(t; t_w, \omega)$ are equal in magnitude, but this common value reaches its highest point when $t_w = \tau$.

Figure 6(b) presents $\Delta(t; t_w, \omega)$ for $\tau = t_w = 0.36$ and five values of ω : 0.44, 0.58, 0.60, 0.62, and 0.65. For these parameters, a Mpemba effect occurs if $\kappa_0^{-1} \simeq 0.45 < \omega < 1 - \tau = 0.64$. This explains why no effect is observed for $\omega = 0.44$ (where $\Delta(t) > 0$ for all t) or $\omega = 0.65$ (where $\Delta(t) < 0$ for all t). Additionally, $\omega = 0.58$ corresponds to a case where the initial positive Δ exceeds the absolute value of its minimum, whereas the opposite occurs for $\omega = 0.62$.

Let us summarize the results thus far. For given values of τ and t_w , the existence of a Mpemba effect requires that the normalized warm temperature ω lies within the interval defined by Eq. (14). Within this interval, the effect is maximal at $\omega = \tilde{\omega}(t_w)$, and the magnitude of this maximal effect is given by $\text{Mp}(t_w)$. Ac-

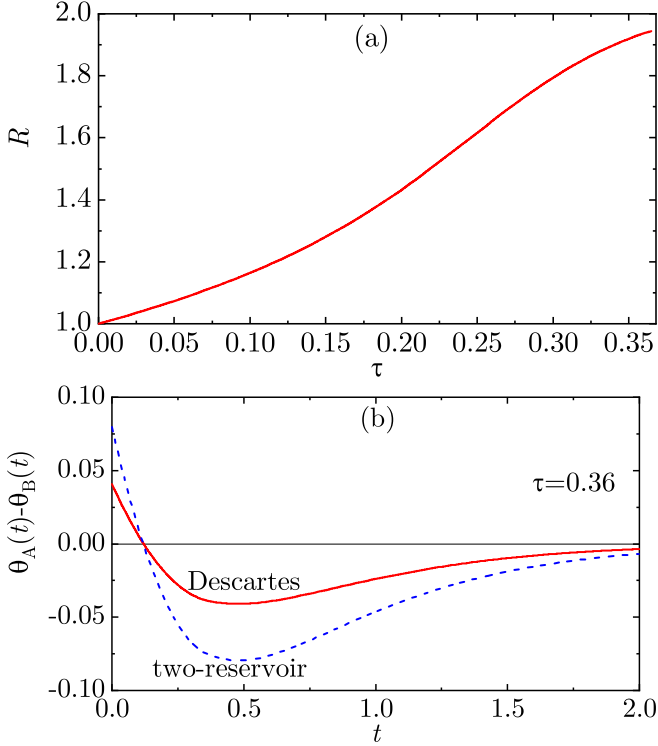


FIG. 7. (a) Ratio between the magnitude of the Mpemba effect in the two-reservoir protocol and the maximum magnitude in the Descartes protocol [see Eq. (38)]. (b) Solid line (Descartes protocol): $\theta_A - \theta_B = \Delta(t; t_w, \omega)$ for $\tau = t_w = 0.36$ and $\omega = \tilde{\omega}(t_w) \simeq 0.60$; dashed line (two-reservoir protocol): $\theta_A - \theta_B = 2\Delta(t; t_w, \omega)$ for $\tau = 0.36$, $\omega = 1/2$, and $t_w = \tilde{t}_w \simeq 0.47$. In both cases the temperature difference is normalized with respect to $T_{\text{hot}} - T_{\text{cold}}$.

curate and practical approximations for both quantities are provided by Eqs. (35) and (36).

3. Maximum magnitude of the Mpemba effect in the Descartes and two-reservoir protocols

Given the delay time τ , we have seen that the maximum magnitude of the Mpemba effect in the Descartes protocol is obtained for $t_w = \tau$ and $\omega = \tilde{\omega}(t_w = \tau)$ [see Eq. (37)].

As noted above, the difference function $\theta_A - \theta_B$ associated with the two-reservoir protocol of Fig. 1(a) is exactly twice that of the Descartes protocol with $\omega = 1/2$ and the same values of τ and t_w . This comparison is made using the same definition of the difference function, normalized with respect to the extreme temperature difference $T_{\text{hot}} - T_{\text{cold}}$ [see Eq. (8)]. For that value of the normalized warm temperature, the optimal Mpemba effect is obtained with a waiting time $t_w = \tilde{t}_w$, where \tilde{t}_w is the solution to $\tilde{\omega}(\tilde{t}_w) = 1/2$.

To compare the magnitudes of the Mpemba effect in the two-reservoir and the Descartes protocols, we intro-

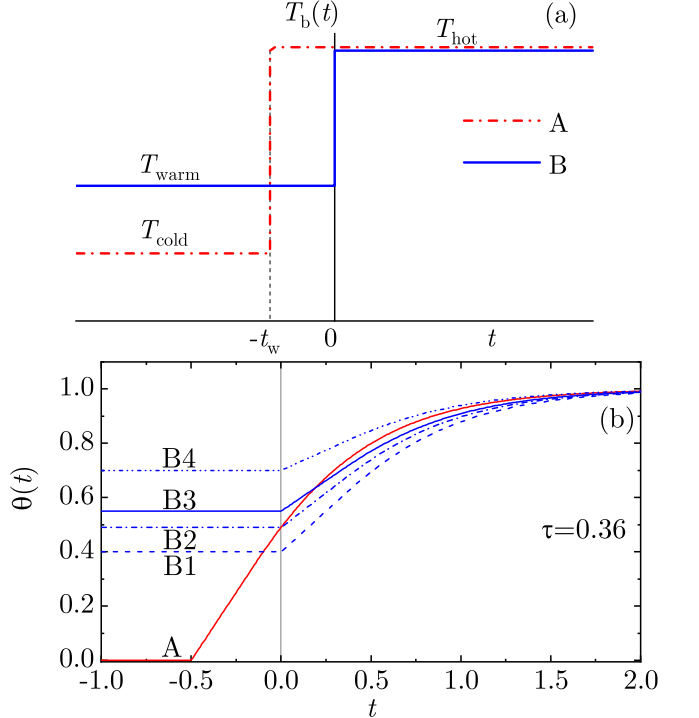


FIG. 8. (a) Schematic representation of the Descartes heating protocol. (b) Normalized temperature $\theta(t)$ for a sample of type A and different samples of type B with delay time $\tau = 0.36$. The waiting time is $t_w = 0.5$ for sample A, while the normalized warm temperature is $\omega = 0.40, 0.49, 0.55$, and 0.70 for samples B1, B2, B3, and B4, respectively.

duce the ratio

$$R = 2 \frac{\text{Mp}(t_w = \tilde{t}_w)}{\text{Mp}(t_w = \tau)}. \quad (38)$$

It is plotted in Fig. 7(a) as a function of the delay time τ . We observe that, even though the Descartes protocol includes ω as an additional control parameter, its maximum Mpemba magnitude is always smaller than that of the two-reservoir protocol with the same delay time. This is further illustrated in Fig. 7(b) for $\tau = 0.36$.

III. THE DESCARTES HEATING PROTOCOL FOR THE INVERSE MPEMBA EFFECT

While the Descartes protocol was originally proposed for the conventional cooling scenario, it can be straightforwardly adapted to the heating case. In this variant, sample A remains in thermal equilibrium with a reservoir at a cold temperature T_{cold} until time $t = -t_w$, when it is quenched to a hot temperature T_{hot} . Sample B is equilibrated with a reservoir at an intermediate warm temperature T_{warm} until $t = 0$, when it is also quenched to the same hot temperature T_{hot} as sample A. This heating protocol is sketched in Fig. 8(a). If the initial post-quench temperatures satisfy $T_A(0) < T_B(0)$,

an inverse Mpemba effect takes place provided that $T_A(t_x) = T_B(t_x)$ at some crossover time t_x , and subsequently $T_A(t) > T_B(t)$ for $t > t_x$.

The equations for the heating process can be obtained from those of the cooling process by performing the formal change $T_{\text{cold}} \leftrightarrow T_{\text{hot}}$. In particular, from Eq. (9) one obtains

$$\frac{T_B(t) - T_A(t)}{T_{\text{hot}} - T_{\text{cold}}} = \bar{\Delta}(t; t_w, \omega), \quad t \geq 0, \quad (39)$$

where ω is still defined by Eq. (2) and the difference function is now

$$\begin{aligned} \bar{\Delta}(t; t_w, \omega) &= \Delta(t; t_w, 1 - \omega) \\ &= \mathcal{E}(t + t_w) - (1 - \omega)\mathcal{E}(t). \end{aligned} \quad (40)$$

The condition for the existence of an inverse Mpemba effect follows from Eq. (14) with the replacement $\omega \rightarrow 1 - \omega$:

$$1 - \mathcal{E}(t_w) < \omega < 1 - e^{-\kappa_0 t_w}. \quad (41)$$

The rest of the results presented in Sec. II remain valid, except for the replacement $\omega \rightarrow 1 - \omega$. In particular, Fig. 8(b) represents the counterpart of Fig. 2(a). For $\tau = 0.36$ and $t_w = 0.5$, the bounds of the inverse Mpemba interval are $1 - \mathcal{E}(t_w) \simeq 0.49$ and $1 - e^{-\kappa_0 t_w} \simeq 0.67$. This agrees with Fig. 8, where an inverse Mpemba effect is observed for $\omega = 0.55$, but not for $\omega = 0.40$ or $\omega = 0.70$. The case $\omega = 0.49$ corresponds to the heating version of the genuine Descartes protocol, where $T_A(0) = T_B(0) = T_{\text{warm}}$.

IV. INFLUENCE OF FINITE-RATE QUENCHES

Thus far, we have assumed that, in the Descartes cooling protocol, the bath temperatures experience *instantaneous* quenches from T_{hot} to T_{cold} at $t = -t_w$ (in the case of sample A) and from T_{warm} to T_{cold} at $t = 0$ (in the case of sample B). However, it is more realistic to assume that the quenches take place at a finite rate with a characteristic time σ [62], i.e.,

$$T_{b,A}(t) = \begin{cases} T_{\text{hot}}, & t \leq -t_w, \\ T_{\text{cold}} + (T_{\text{hot}} - T_{\text{cold}}) e^{-(t+t_w)/\sigma}, & t \geq -t_w, \end{cases} \quad (42a)$$

$$T_{b,B}(t) = \begin{cases} T_{\text{warm}}, & t \leq 0, \\ T_{\text{cold}} + (T_{\text{warm}} - T_{\text{cold}}) e^{-t/\sigma}, & t \geq 0. \end{cases} \quad (42b)$$

Consequently, for $t \geq 0$,

$$\frac{T_{b,A}(t) - T_{b,B}(t)}{T_{\text{hot}} - T_{\text{cold}}} = (e^{-t_w/\sigma} - \omega) e^{-t/\sigma}, \quad t \geq 0. \quad (43)$$

The corresponding time-dependence of the temperature samples is again given by Eq. (3), except that the function $\mathcal{E}(t)$ is now replaced by [62]

$$\mathcal{E}_\sigma(t) = \mathcal{E}(t) + \mathcal{F}_\sigma(t), \quad (44)$$

where the function $\mathcal{F}_\sigma(t)$ is given by

$$\mathcal{F}_\sigma(t) = - \sum_{n=0}^{\lfloor t/\tau \rfloor} \sigma^{n+1} R_n((t - n\tau)/\sigma), \quad (45a)$$

$$R_n(x) \equiv e^{-x} - \sum_{k=0}^n \frac{(-x)^k}{k!}. \quad (45b)$$

A practical approximate form for $\mathcal{E}_\sigma(t)$ is

$$\begin{aligned} \mathcal{E}_\sigma(t) &\approx \frac{\kappa_0^{-1} e^{-\kappa_0 t}}{(1 - \kappa_0 \sigma)(1 - \kappa_0 \tau)} + \frac{\sigma e^{-t/\sigma}}{\sigma e^{\tau/\sigma} - 1} \\ &\quad - \frac{\kappa_1^{-1} e^{-\kappa_1 t}}{(1 - \kappa_1 \sigma)(\kappa_1 \tau - 1)}, \quad t \gg 1. \end{aligned} \quad (46)$$

This expression reduces to Eq. (6) in the limit of instantaneous quenches ($\sigma = 0$). In the long-time limit, the first term dominates over the second one if $\kappa_0 \sigma < 1$, whereas the opposite occurs if $\kappa_0 \sigma > 1$.

The relative temperature difference for $t \geq 0$ is given by a straightforward extension of Eq. (9):

$$\frac{T_A(t) - T_B(t)}{T_{\text{hot}} - T_{\text{cold}}} = \Delta_\sigma(t; t_w, \omega), \quad t \geq 0, \quad (47a)$$

$$\Delta_\sigma(t; t_w, \omega) = \mathcal{E}_\sigma(t + t_w) - \omega \mathcal{E}_\sigma(t). \quad (47b)$$

From Eq. (46), we see that the asymptotic form of $\Delta_\sigma(t)$ is

$$\begin{aligned} \Delta_\sigma(t; t_w, \omega) &\approx \frac{\kappa_0^{-1} (e^{-\kappa_0 t_w} - \omega) e^{-\kappa_0 t}}{(1 - \kappa_0 \sigma)(1 - \kappa_0 \tau)} + \frac{\sigma (e^{-t_w/\sigma} - \omega) e^{-t/\sigma}}{\sigma e^{\tau/\sigma} - 1} \\ &\quad - \frac{\kappa_1^{-1} (e^{-\kappa_1 t_w} - \omega) e^{-\kappa_1 t}}{(1 - \kappa_1 \sigma)(\kappa_1 \tau - 1)}, \quad t \gg 1. \end{aligned} \quad (48)$$

Following a reasoning similar to that of Sec. II, one finds that the condition for the existence of a direct Mpemba effect changes from Eq. (14) to

$$e^{-t_w \min(\kappa_0, \sigma^{-1})} < \omega < \mathcal{E}_\sigma(t_w). \quad (49)$$

Since $\mathcal{E}_\sigma(t) > \mathcal{E}(t)$, Eq. (49) suggests that the window of values of the normalized warm temperature ω for which a Mpemba effect exists widens as σ departs from 0. However, this is misleading because, as shown by Eq. (43), the environmental conditions for samples A and B are, in general, different if $\sigma \neq 0$.

An unbiased Mpemba effect would require $T_{b,A}(t) = T_{b,B}(t)$ for $t > 0$, but this is only possible (apart from the case $\sigma = 0$) if the waiting time t_w and the quench characteristic time σ are coupled by

$$t_w = \sigma \ln \omega^{-1}. \quad (50)$$

It can be checked that $\omega^{-1} \mathcal{E}_\sigma(t_w = \sigma \ln \omega^{-1})$ is always larger than 1, so that, if $t_w = \sigma \ln \omega^{-1}$, the upper bound

in Eq. (49) is satisfied for any τ and ω . Let us see that, on the other hand, the lower bound is incompatible with Eq. (50). The first inequality in Eq. (49) is equivalent to $t_w \min(\kappa_0, \sigma^{-1}) > \ln \omega^{-1}$. Inserting Eq. (50), this condition becomes $\min(\kappa_0 \sigma, 1) > 1$, which is impossible to satisfy.

To reach the same conclusion from an alternative viewpoint, note that the origin of the first inequality in Eq. (49) lies in the condition

$$\lim_{t \rightarrow \infty} \Delta_\sigma(t; t_w, \omega) < 0. \quad (51)$$

In the special case of Eq. (50), the second term on the right-hand side of Eq. (48) vanishes identically, so that

$$\lim_{t \rightarrow \infty} \frac{\Delta_\sigma(t; \sigma \ln \omega^{-1}, \omega)}{e^{-\kappa_0 t}} = \frac{\kappa_0^{-1}}{1 - \kappa_0 \tau} \frac{\omega^{\kappa_0 \sigma} - \omega}{1 - \kappa_0 \sigma}. \quad (52)$$

Since $\omega < 1$, the right-hand side of Eq. (52) is strictly positive, thus contradicting the condition in Eq. (51).

While, strictly speaking, a Mpemba effect is not possible with finite-rate quenches because of the physical requirement of equal bath conditions for both samples, the differences in the environmental conditions become negligible within a tolerable range if σ is sufficiently small. This approximate equivalence allows the Mpemba effect observed under instantaneous quenches to persist, albeit imperfectly [61].

V. CONCLUSIONS

In this work, the direct and inverse Mpemba effects have been investigated within the framework of the time-delayed Newton's law of cooling by means of the Descartes protocol, a three-reservoir scheme in which each sample undergoes a single thermal quench at different times. This protocol allows one to disentangle the roles of the delay time τ , the waiting time t_w , and the normalized warm temperature ω , providing a transparent and flexible setting to analyze the phenomenon.

For instantaneous quenches, we have derived exact conditions for the existence of both the direct and inverse Mpemba effects, expressed as bounds on ω for given τ and t_w . Within those bounds, the effect becomes maximal at a specific value $\omega = \tilde{\omega}(t_w)$, determined by the condition that the initial difference equals in magnitude the subsequent minimum of $\Delta(t; t_w, \omega)$. At this optimum, the Mpemba magnitude is defined by this common extremal value. Practical and accurate approximations for both $\tilde{\omega}(t_w)$ and the maximal magnitude $Mp(t_w)$ have been obtained, leading to compact

expressions that do not require the numerical solution of transcendental equations. A particularly relevant result is that the absolute maximum of the Mpemba effect at fixed τ is reached for $t_w = \tau$.

The Descartes protocol has also been compared with the previously studied two-reservoir protocol. Although the Descartes scheme introduces ω as an additional control parameter, the maximum attainable magnitude of the Mpemba effect is found to be systematically smaller than that of the two-reservoir protocol with the same delay time. This comparison clarifies the relative efficiency of both protocols and highlights the non-trivial interplay between the number of reservoirs and the achievable strength of the effect.

The analysis has been extended to the more realistic situation of finite-rate quenches characterized by a bath time scale σ . While finite-rate quenches formally enlarge the interval of ω values for which a sign change in $\Delta(t)$ may occur, the requirement of identical bath conditions for both samples after $t = 0$ imposes a coupling between t_w and σ that ultimately precludes a strict Mpemba effect. Nevertheless, when σ is sufficiently small, the environmental differences become negligible and the behavior approaches that of the instantaneous-quench limit, so that an approximate Mpemba effect can still be observed.

Overall, the Descartes protocol provides a unified and analytically tractable framework to characterize the Mpemba effect and its inverse counterpart, as well as to quantify their magnitude and parametric dependence. The methodology developed here can be naturally applied to other multi-step thermal protocols. In particular, a systematic study of the Pontus protocol using the same analytical tools appears as a promising direction for future work, which may further clarify the influence of protocol structure and reservoir sequencing on the emergence and strength of anomalous thermal relaxation.

ACKNOWLEDGMENTS

I acknowledge financial support from Grant No. PID2024-156352NB-I00 funded by MCIU/AEI/10.13039/501100011033/FEDER, UE, and from Grant No. GR24022 funded by the Junta de Extremadura (Spain) and by European Regional Development Fund (ERDF) "A way of making Europe."

[1] Aristotle, *The Works of Aristotle (Translated into English under the editorship of W.D. Ross)*, Vol. III, edited by W. D.

Ross (Clarendon Press, Oxford, 1931).
[2] E. B. Mpemba and D. G. Osborne, Cool?,

Phys. Educ. **4**, 172 (1969).

[3] G. S. Kell, The freezing of hot and cold water, *Am. J. Phys.* **37**, 564 (1969).

[4] I. Firth, Cooler?, *Phys. Educ.* **6**, 32 (1971).

[5] E. Deeson, Cooler-lower down, *Phys. Educ.* **6**, 42 (1971).

[6] J. Walker, Hot water freezes faster than cold water. Why does it do so?, *Sci. Am.* **237**, 246 (1977).

[7] M. Freeman, Cooler still—an answer?, *Phys. Educ.* **14**, 417 (1979).

[8] B. Wojciechowski, I. Owczarek, and G. Bednarz, Freezing of aqueous solutions containing gases, *Cryst. Res. Technol.* **23**, 843 (1988).

[9] D. Auerbach, Supercooling and the Mpemba effect: When hot water freezes quicker than cold, *Am. J. Phys.* **63**, 882 (1995).

[10] P. K. Maciejewski, Evidence of a convective instability allowing warm water to freeze in less time than cold water, *J. Heat Transf.* **118**, 65 (1996).

[11] S. Esposito, R. De Risi, and L. Somma, Mpemba effect and phase transitions in the adiabatic cooling of water before freezing, *Physica A* **387**, 757 (2008).

[12] J. I. Katz, When hot water freezes before cold, *Am. J. Phys.* **77**, 27 (2009).

[13] M. Vynnycky and S. L. Mitchell, Evaporative cooling and the Mpemba effect, *Heat Mass Transf.* **46**, 881 (2010).

[14] M. Vynnycky and N. Maeno, Axisymmetric natural convection-driven evaporation of hot water and the Mpemba effect, *Intl. J. Heat Mass Transf.* **55**, 7297 (2012).

[15] X. Zhang, Y. Huang, Z. Ma, Y. Zhou, J. Zhou, W. Zheng, Q. Jiang, and C. Q. Sun, Hydrogen-bond memory and water-skin supersolidity resolving the Mpemba paradox, *Phys. Chem. Chem. Phys.* **16**, 22995 (2014).

[16] M. Vynnycky and S. Kimura, Can natural convection alone explain the Mpemba effect?, *Intl. J. Heat Mass Transf.* **80**, 243 (2015).

[17] J. Jin and W. A. Goddard, Mechanisms underlying the Mpemba effect in water from molecular dynamics simulations, *J. Phys. Chem. C* **119**, 2622 (2015).

[18] R. T. Ibekwe and J. P. Cullerne, Investigating the Mpemba effect: When hot water freezes faster than cold water, *Phys. Educ.* **51**, 025011 (2016).

[19] C. Q. Sun, Y. L. Huang, X. Zhang, Z. S. Ma, and B. Wang, The physics behind water irregularity, *Phys. Rep.* **998**, 1 (2023).

[20] G. Teza, J. Bechhoefer, A. Lasanta, O. Raz, and M. Vucelja, Speedups in nonequilibrium thermal relaxation: Mpemba and related effects, *Phys. Rep.* **1164**, 1 (2026).

[21] A. Lasanta, F. Vega Reyes, A. Prados, and A. Santos, When the hotter cools more quickly: Mpemba effect in granular fluids, *Phys. Rev. Lett.* **119**, 148001 (2017).

[22] A. Torrente, M. A. López-Castaño, A. Lasanta, F. Vega Reyes, A. Prados, and A. Santos, Large Mpemba-like effect in a gas of inelastic rough hard spheres, *Phys. Rev. E* **99**, 060901(R) (2019).

[23] A. Biswas, V. V. Prasad, O. Raz, and R. Rajesh, Mpemba effect in driven granular Maxwell gases, *Phys. Rev. E* **102**, 012906 (2020).

[24] E. Mompó, M. A. López-Castaño, A. Torrente, F. Vega Reyes, and A. Lasanta, Memory effects in a gas of viscoelastic particles, *Phys. Fluids* **33**, 062005 (2021).

[25] R. Gómez González, N. Khalil, and V. Garzó, Mpemba-like effect in driven binary mixtures, *Phys. Fluids* **33**, 053301 (2021).

[26] R. Gómez González and V. Garzó, Time-dependent homogeneous states of binary granular suspensions, *Phys. Fluids* **33**, 093315 (2021).

[27] A. Biswas, V. V. Prasad, and R. Rajesh, Mpemba effect in an anisotropically driven granular gas, *EPL* **136**, 46001 (2021).

[28] A. Biswas, V. V. Prasad, and R. Rajesh, Mpemba effect in anisotropically driven inelastic Maxwell gases, *J. Stat. Phys.* **186**, 45 (2022).

[29] A. Megías and A. Santos, Kinetic theory and memory effects of homogeneous inelastic granular gases under nonlinear drag, *Entropy* **24**, 1436 (2022).

[30] A. Megías and A. Santos, Mpemba-like effect protocol for granular gases of inelastic and rough hard disks, *Front. Phys.* **10**, 971671 (2022).

[31] A. Patrón, B. Sánchez-Rey, C. A. Plata, and A. Prados, Non-equilibrium memory effects: Granular fluids and beyond, *EPL* **143**, 61002 (2023).

[32] M. Baity-Jesi, E. Calore, A. Cruz, L. A. Fernandez, J. M. Gil-Narvío, A. Gordillo-Guerrero, D. Iñiguez, A. Lasanta, A. Maiorano, E. Marinari, V. Martín-Mayor, J. Moreno-Gordo, A. Muñoz-Sudupe, D. Navarro, G. Parisi, S. Perez-Gaviro, F. Ricci-Tersenghi, J. J. Ruiz-Lorenzo, S. F. Schifano, B. Seoane, A. Tarancón, R. Tripiccione, and D. Yllanes, The Mpemba effect in spin glasses is a persistent memory effect, *Proc. Natl. Acad. Sci. U.S.A.* **116**, 15350 (2019).

[33] I. González-Adalid Pemartín, E. Mompó, A. Lasanta, V. Martín-Mayor, and J. Salas, Slow growth of magnetic domains helps fast evolution routes for out-of-equilibrium dynamics, *Phys. Rev. E* **104**, 044114 (2021).

[34] N. Vadakkayila and S. K. Das, Should a hotter paramagnet transform quicker to a ferromagnet? Monte Carlo simulation results for Ising model, *Phys. Chem. Chem. Phys.* **23**, 11186 (2021).

[35] G. Teza, R. Yaacoby, and O. Raz, Eigenvalue crossing as a phase transition in relaxation dynamics, *Phys. Rev. Lett.* **130**, 207103 (2023).

[36] G. Teza, R. Yaacoby, and O. Raz, Relaxation shortcuts through boundary coupling, *Phys. Rev. Lett.* **131**, 017101 (2023).

[37] S. K. Das, Perspectives on a few puzzles in phase transformations: When should the farthest reach the earliest?, *Langmuir* **39**, 10715 (2023).

[38] I. González-Adalid Pemartín, E. Mompó, A. Lasanta, V. Martín-Mayor, and J. Salas, Shortcuts of freely relaxing systems using equilibrium physical observables, *Phys. Rev. Lett.* **132**, 117102 (2024).

[39] A. Kumar and J. Bechhoefer, Exponentially faster cooling in a colloidal system, *Nature (Lond.)* **584**, 64 (2020).

[40] J. Bechhoefer, A. Kumar, and R. Chétrite, A fresh understanding of the Mpemba effect, *Nat. Rev. Phys.* **3**, 534 (2021).

[41] R. Chétrite, A. Kumar, and J. Bechhoefer, The metastable Mpemba effect corresponds to a non-monotonic temperature dependence of extractable work, *Front. Phys.* **9**, 654271 (2021).

[42] A. Kumar, R. Chétrite, and J. Bechhoefer, Anomalous heating in a colloidal system, *Proc. Natl. Acad. Sci. U.S.A.* **119**, e2118484119 (2022).

[43] M. Ibáñez, C. Dieball, A. Lasanta, A. Godec, and A. Rica, Heating and cooling are fundamentally asymmetric and evolve along distinct pathways, *Nature Phys.* **20**, 135 (2024).

[44] Z. Lu and O. Raz, Nonequilibrium thermodynam-

ics of the Markovian Mpemba effect and its inverse, *Proc. Natl. Acad. Sci. U.S.A.* **114**, 5083 (2017).

[45] I. Klich, O. Raz, O. Hirschberg, and M. Vucelja, Mpemba index and anomalous relaxation, *Phys. Rev. X* **9**, 021060 (2019).

[46] D. M. Busiello, D. Gupta, and A. Maritan, Inducing and optimizing Markovian Mpemba effect with stochastic reset, *New J. Phys.* **23**, 103012 (2021).

[47] J. Lin, K. Li, J. He, J. Ren, and J. Wang, Power statistics of Otto heat engines with the Mpemba effect, *Phys. Rev. E* **105**, 014104 (2022).

[48] F. Carollo, A. Lasanta, and I. Lesanovsky, Exponentially accelerated approach to stationarity in Markovian open quantum systems through the Mpemba effect, *Phys. Rev. Lett.* **127**, 060401 (2021).

[49] A. K. Chatterjee, S. Takada, and H. Hayakawa, Quantum Mpemba effect in a quantum dot with reservoirs, *Phys. Rev. Lett.* **131**, 080402 (2023).

[50] A. K. Chatterjee, S. Takada, and H. Hayakawa, Multiple quantum Mpemba effect: exceptional points and oscillations, *Phys. Rev. A* **110**, 022213 (2024).

[51] S. Murciano, F. Ares, I. Klich, and P. Calabrese, Entanglement asymmetry and quantum Mpemba effect in the XY spin chain, *J. Stat. Mech.* **2024**, 013103 (2024).

[52] L. K. Joshi, J. Franke, A. Rath, F. Ares, S. Murciano, F. Kranzl, R. Blatt, P. Zoller, B. Vermersch, P. Calabrese, C. F. Roos, and M. K. Joshi, Observing the quantum Mpemba effect in quantum simulations, *Phys. Rev. Lett.* **133**, 010402 (2024).

[53] S. A. Shapira, Y. Shapira, J. Markov, G. Teza, N. Akerman, O. Raz, and R. Ozeri, The Mpemba effect demonstrated on a single trapped ion qubit, *Phys. Rev. Lett.* **133**, 010403 (2024).

[54] X. Wang and J. Wang, Mpemba effects in nonequilibrium open quantum systems, *Phys. Rev. Res.* **6**, 033330 (2024).

[55] F. Caceffo, S. Murciano, and V. Alba, Entangled multiplets, asymmetry, and quantum Mpemba effect in dissipative systems, *J. Stat. Mech.* **2024**, 063103 (2024).

[56] S. Yamashika, F. Ares, and P. Calabrese, Entanglement asymmetry and quantum Mpemba effect in two-dimensional free-fermion systems, *Phys. Rev. B* **110**, 085126 (2024).

[57] S. Liu, H.-K. Zhang, S. Yin, and S.-X. Zhang, Symmetry restoration and quantum Mpemba effect in symmetric random circuits, *Phys. Rev. Lett.* **133**, 140405 (2024).

[58] D. J. Strachan, A. Purkayastha, and S. R. Clark, Non-Markovian quantum Mpemba effect, *Phys. Rev. Lett.* **134**, 220403 (2025).

[59] A. Nava and R. Egger, Pontus-Mpemba effects, *Phys. Rev. Lett.* **135**, 140404 (2025).

[60] N. Hatime, S. Melliani, A. E. Mfadel, D. Baleanu, and M. Elomari, Existence, uniqueness, and finite-time stability of solutions for Ψ -Caputo fractional differential equations with time delay, *Comput. Methods Differ. Equ.* **11**, 785 (2023).

[61] A. Santos, Mpemba meets Newton: Exploring the Mpemba and Kovacs effects in the time-delayed cooling law, *Phys. Rev. E* **109**, 044149 (2024).

[62] A. Santos, Time-delayed Newton's law of cooling with a finite-rate thermal quench: Impact on the Mpemba and Kovacs effects, *Phys. Rev. E* **111**, 055402 (2025).

[63] A. Nava, R. Egger, B. Dey, and D. Giuliano, Speeding up Pontus-Mpemba effects via dynamical phase transitions, *Phys. Rev. Res.* **7**, 043332 (2025).

[64] R. Descartes, *The Philosophical Writings of Descartes, vol. III: The Correspondence*. (Cambridge Univ. Press, Cambridge, 1991) translated by J. Cottingham, R. Stoothoff, D. Murdoch, and A. Kenny.

[65] R. M. Corless, G. H. Gonnet, D. E. G. Hare, D. J. Jeffrey, and D. E. Knuth, On the lambert W function, *Adv. Comput. Math.* **5**, 329 (1996).